Molecular Immunology 105 (2019) 46–54

Contents lists available at ScienceDirect

Molecular Immunology

journal homepage: www.elsevier.com/locate/molimm

The lncRNA H19/miR-675 axis regulates myocardial ischemic and reperfusion injury by targeting PPARα

Hong Luo[a,*], Jing Wang[b], Donghai Liu[a], Suhua Zang[a], Ning Ma[a], Lixuan Zhao[a], Liang Zhang[a], Xin Zhang[a], Chenhui Qiao[a]

[a] Department of Cardiovascular Surgery, The First Affiliated Hospital of Zhengzhou University, Zhengzhou, Henan, 450052, China
[b] Department of Stomatology, The First Affiliated Hospital of Zhengzhou University, Zhengzhou, Henan, 450052, China

ARTICLE INFO

Keywords:
lncRNA H19
miR-675
Myocardial ischemic-reperfusion injury
Apoptosis
Inflammation
PPARα

ABSTRACT

Increasing evidence has indicated that lncRNAs and miRNAs play important roles in the pathogenesis of myocardial ischemic and reperfusion (I/R) injury. This study investigated the potential roles and underlying molecular mechanisms of lncRNA H19 and H19-derived miR-675 in regulating myocardial I/R injury in vitro and in vivo. The results showed that expression of H19 and H19-derived miR-675 was upregulated in cardiomyocytes exposed to oxygen-glucose deprivation and reperfusion. Knockdown of H19 increased cell viability, reduced cell apoptosis, decreased inflammatory cytokines (IL-1β, TNF-α and IL-6), inhibited oxidative stress, downregulated p-IκB-α and p-p65, and upregulated expression of Nrf2 and HO-1. All of these effects were partly reversed by overexpression of miR-675. Furthermore, we found that PPARα was a target gene of miR-675 and that H19 negatively regulated PPARα expression via miR-675. By inhibiting PPARα, the biological effects of miR-675 or H19 inhibition on cellular functions (apoptosis, inflammation and oxidative stress) were at least partially reversed. Moreover, knockdown of H19 significantly reduced infarct size, increased left ventricular systolic pressure, and decreased left ventricular end-diastolic pressure in a mouse model of myocardial I/R. Taken together, these data indicate that H19 inhibition protects the heart against myocardial I/R injury, which may be partly attributed to regulation of the miR-675/PPARα axis.

1. Introduction

Myocardial infarction (MI) is a major cause of death and disability worldwide. It results from thrombus, which prevents blood flow to the metabolically highly active myocardium. The most effective therapy to limit infarct size and reduce MI injury is the rapid restoration of blood flow through the occluded coronary artery via mechanical or pharmacological intervention (Liao et al., 2016). However, myocardial reperfusion can induce additional cardiomyocyte death and increase infarct size, a phenomenon called myocardial ischemia and reoxygenation (I/R) injury, for which there is still no effective therapy (Hausenloy and Yellon, 2013). Thus, I/R injury remains a crucial therapeutic target for cardiac protection in patient with MI.

Recently, increasing evidence has suggested that noncoding transcripts are functionally active as physiological and pathological regulation molecules. These noncoding RNAs include the well-known microRNAs (miRNAs) and the recently acknowledged long noncoding RNAs (lncRNAs). LncRNAs are transcripts longer than 200 nucleotides that regulate various biological processes by interacting with multiple molecules, including DNA, RNA, and proteins. MiRNAs are single-stranded RNAs that are 18–22 nucleotides long. MiRNAs regulate genes by binding to the 3′ untranslated regions (UTRs) of target mRNAs, which leads to mRNA degradation or mRNA translation inhibition. Studies have indicated that noncoding RNAs are involved in regulating heart diseases, including myocardial I/R (Ong et al., 2018; Wang et al., 2015a; Zhao et al., 2017). Thus, it is urgent to identify lncRNAs and define their functions in myocardial I/R.

The lncRNA H19 gene belongs to a highly conserved, imprinted gene cluster. It is deeply involved in embryonic development and growth control (Gabory et al., 2010). H19 expression is mainly induced during embryogenesis and decreases after birth, except in adult skeletal and heart muscle (Li et al., 2016). It has been reported that H19 is a primary miRNA precursor for microRNA-675 (miR-675) (Cai and Cullen, 2007). The H19 and miR-675 axis has been found to be critically involved in several diseases, such as tumorigenesis (Tsang et al., 2010; Vennin et al., 2015), chronic obstructive pulmonary disease (Lewis et al., 2016) and diabetic cardiomyopathy (Li et al., 2016), suggesting that the function of H19 in some biological processes is

* Corresponding author.
E-mail address: hongluo_lh@163.com (H. Luo).

https://doi.org/10.1016/j.molimm.2018.11.011
Received 14 May 2018; Received in revised form 24 October 2018; Accepted 14 November 2018
Available online 26 November 2018
0161-5890/ © 2018 Elsevier Ltd. All rights reserved.

mediated via miR-675. However, whether the H19/miR-675 axis participates in regulating myocardial I/R injury remains unknown.

In the present study, we aimed to determine the role and underlying molecular mechanisms of the H19/miR-675 axis in two models, a cellular model of oxygen-glucose deprivation/reperfusion (OGD/R) in cardiomyocytes and a mouse model of myocardial I/R in C57BL/6 mice. Respectively, these models provide in vitro and in vivo theoretical support to clarify the involvement of this axis in myocardial I/R injury. Our data indicate that the H19/miR-675 axis may be an effective therapeutic target for protecting the heart from myocardial I/R injury.

2. Materials and methods

2.1. Cardiomyocyte culture and OGD/R treatment

The isolation and culture of primary cardiomyocytes was performed as described previously (Wang et al., 2015b) with minor modifications. Briefly, the hearts were surgically removed from male mice aged 1–2 days and immediately washed in cold HEPES (4-[2-hydroxyethyl]-1-piperazineethanesulfonic acid) buffer saline solution. The ventricular tissues were cut into small pieces and dispersed in a series of digestion at 37 °C in HEPES-buffered saline solution containing pancreatin at a concentration of 1.2 mg/mL and collagenase (Gibco, Grand Island, NY, USA) at a concentration of 0.14 mg/mL. After centrifugation, the cells were suspended in Dulbecco's Modified Eagle's medium (Gibco) containing 20% calf serum, penicillin (100 U/ml), and streptomycin (100 mg/ml). The dissociated cells were pre-plated at 37 °C for 1 h to separate cardiomyocytes by adherence of cardiac fibroblasts. Then, the cells were collected and diluted to 1×10^6 cells/ml and plated in different culture dishes according to the specific experimental requirements. Cardiomyocytes were incubated at 37 °C in a humidified atmosphere containing 5% CO_2.

OGD/R was induced as follows. The cells were cultured in an ischemia-mimetic solution (140 NaCl mmol/L, 3.5 KCl mmol/L, 0.43 KH2PO4 mmol/L, 1.25 MgSO4 mmol/L, 1.7 CaCl2 mmol/L, and 5 NaHCO3 mmol/L; 20 HEPES; pH 7.2 to pH 7.4) as previously described (Wang et al., 2017). The cells were kept in a hypoxic incubator chamber with 95% N_2 and 5% CO_2 at 37 °C for 2 h, 4 h, or 6 h. For reperfusion, the cells were transferred to normal culture medium and incubated in 95% O_2 and 5% CO_2 at 37 °C for 24 h (Wang et al., 2017).

2.2. Cell transfection

Small interference RNA (siRNA) against H19, PPARα, the miR-675 mimic, the miR-675 inhibitor, or the negative control were synthesized by GenePharma Co., Ltd. (Shanghai, China). The siRNA, miRNA mimic, or miRNA inhibitor was transfected into cells by Lipofectamine 2000 (Invitrogen, Carlsbad, CA, USA) according to the manufacturer's instructions. After 24 h of transfection, OGD/R was induced for further analysis.

2.3. Detection of lactate dehydrogenase

The level of LDH was examined using a LDH assay kit (Jiancheng Biotech, Nanjing, China) according to the manufacturer's protocols.

2.4. Cell viability assay

The viability of cardiomyocytes was determined using a CCK-8 detection kit (Beyotime, Shanghai, China). Ten μl of CCK-8 solution was added to each well of the culture medium. The absorbance value was measured at 450 nm using a microplate reader (ThermoFisher Scientific, Waltham, MA, USA).

2.5. Cell apoptosis assay

Cardiomyocyte apoptosis was detected with an Annexin V-FITC apoptosis detection kit (Beyotime) according to the manufacturer's instructions. Briefly, the cells were stained with Annexin V-FITC and propidium iodide (PI) and then subjected to flow cytometry to detect apoptosis.

2.6. Inflammatory cytokines detection

Concentrations of inflammatory markers tumor necrosis factor-α (TNF-α), interleukin-1β (IL-1β), and interleukin-6 (IL-6) were measured using commercial enzyme-linked immunosorbent assay (ELISA) kits (R &D Systems, Minneapolis, MN, USA) according to the manufacturer's protocol.

2.7. Oxidative stress measurement

Oxidative stress was assessed by detecting malondialdehyde (MDA) and superoxide dismutase (SOD) detection kits (Jiancheng Biotech) according to the manufacturer's instructions. ROS levels were determined by using 2′,7′-dichlorodihydrofluorescein diacetate (DCHF-DA) probes. In brief, cells were incubated with 10 μM of DCHF-DA for 20 min and then analyzed by flow cytometry.

2.8. Quantitative PCR (qPCR)

Total RNA was isolated from cardiomyocytes and myocardial tissues using TRIzol Reagent (Invitrogen) according to the manufacturer's instructions. RNA was reverse transcribed to cDNA using SuperScript First Strand cDNA System (Invitrogen). A qPCR was conducted using SYBR Premix Ex Taq kit (Takara, Dalian, China) on an Applied Biosystems 7500 Real-Time PCR System. For H19 detection, GAPDH was used as the endogenous control. For miR-675 detection, U6 was used as an endogenous reference. The relative expression of H19 and miR-675 was calculated using the $2^{-\Delta\Delta Ct}$ method.

2.9. Western blot

Protein homogenates were prepared from cardiomyocytes and myocardial tissues using RIPA protein extraction reagent supplemented with 1 mM of phenylmethanesulfonyl fluoride. Equal amounts (50 μg) of protein were separated by SDS-PAGE and transferred onto nitrocellulose membranes (Millipore, Billerica, MA, USA). After blocking in 5% non-fat milk, the membranes were incubated with primary antibodies at 4 °C overnight and then incubated with horseradish-peroxidase-conjugated secondary antibodies at room temperature for 1 h. The antibodies were purchased from Cell Signaling Technology (Beverly, MA, USA) or Abcam (Cambridge, MA, USA) and used at the manufacturers' recommended dilutions. The protein bands were visualized using an enhanced chemiluminescence detection kit (Amersham Biosciences, Piscataway, NJ, USA).

2.10. Luciferase reporter assay

The 3′ UTR of PPARα, containing the predicted miR-675 binding site, was amplified by PCR and cloned into the pGL3 luciferase reporter vector to generate the pGL3-PPARα-WT vector. The mutant 3′ UTR sequences without the miR-675 binding site were generated using a QuikChange II XL Site-Directed Mutagenesis Kit (Stratagene, La Jolla, CA, USA) and used to generate the pGL3-PPARα-MUT vector. For the luciferase assay, cells were plated into 96-well plates 24 h prior to transfection and then transfected with either a wild-type or mutant construct and the miR-675 mimic or a negative control. After 48 h of transfection, luciferase activity was detected using the Dual Luciferase Reporter Assay System (Promega, Madison, WI, USA) according to the

manufacturer's instructions.

2.11. Animals and I/R surgery

Male C57BL/6 mice in this experiment weighed 25 g–35 g and were obtained from the Laboratory Animal Center of Zhengzhou University. The mice were raised in a 12-h day and night cycle with free water intake. The feeding room temperature was kept between 18 °C and 25 °C. The Ethics Committee of Zhengzhou University approved all protocols.

Cardiac I/R surgery was performed as previously described (Zhao et al., 2017). In brief, animals were anesthetized with chloral hydrate at a concentration of 30 mg/kg. A thoracotomy was performed on the left side in the fourth intercostal space. After removing the pericardium, the left anterior descending artery at the inferior edge of the left atrium was ligatured with an 8-0 prolene suture. After 45 min of ischemia, the left anterior coronary artery was released and perfused for 1 week (Wang et al., 2015b).

Adenoviruses harboring H19 siRNAs, and their scramble forms were constructed using the pSilencer adeno 1.0-CMV System (Ambion, Austin, TX, USA) according to the kit's instructions. All constructs were amplified in HEK293 cells. The intracoronary delivery of adenoviruses was performed as previously described (Wang et al., 2015b). Five days after the injection of adenoviruses, the mice were subjected to I/R surgery. The left ventricular systolic pressure (LVSP) and left ventricular end-diastolic pressure (LVEDP) were measured on the mice at 1 week after I/R surgery.

2.12. Infarct size determination

Following I/R protocols, the mice were sacrificed, and their hearts were isolated. One part of the heart tissues was used to extract RNA for the mRNA or miRNA detection. Another part was sliced, stained with potassium permanganate and 2,3,5-triphenyltetrazolium chloride (TTC) (Sigma, St. Louis, MO, USA), and fixed to delineate live (red) tissue from dead or infarcted (white) tissue. Infarcts were quantified by planimetry and expressed as a percentage-of-risk zone.

2.13. Statistical analysis

All data are expressed as mean ± SD of at least three independent experiments. The data were analyzed by one-way analysis of variance (ANOVA) followed by the Bonferroni test for multiple comparisons. $P < .05$ was considered statistically significant.

3. Results

3.1. Expression of H19 and miR-675 was upregulated in cardiomyocytes exposed to OGD/R

We built a cellular model of OGD/R using cardiomyocytes to mimic myocardial I/R injury. Compared with the control group, 2 h of oxygen-glucose deprivation, 4 h of oxygen-glucose deprivation, and 6 h of oxygen-glucose deprivation followed by 24 h of reperfusion decreased cell viability and increased LDH (a myocardial injury marker) in a time-dependent manner (Fig. 1A and 1B). H19 expression also was upregulated and showed a 6.79-fold increase in the group with 6 h of oxygen-glucose deprivation followed by 24 h of reperfusion (Fig. 1C). As H19 is a precursor of miR-675, we measured the expression of miR-675 and found a 5.24-fold increase in the group exposed to 6 h of oxygen-glucose deprivation followed by 24 h of reperfusion, compared with the control group (Fig. 1D). Thus, we chose this OGD 6 h/R group for the following experiments. To investigate the roles of H19 in OGD/R injury, the cardiomyocytes were transfected with si-H19 prior to OGD/R, which suppressed the expression of H19 (Fig. 1E). The suppression of H19 further significantly reduced the expression of miR-675 (Fig. 1F). In addition, we measured the levels of miR-103/miR-107, and found that both of them were downregulated in cardiomyocytes exposed to OGD/R (Supplementary Fig. 1).

3.2. The H19/miR-675 axis regulated cell viability and apoptosis in cardiomyocytes exposed to OGD/R

Previous studies have revealed that the H19/miR-675 axis plays a crucial role in various diseases, such as cancers (Guan et al., 2016; Zhu et al., 2014), chronic obstructive pulmonary disease (Lewis et al., 2016) and diabetic cardiomyopathy (Li et al., 2016). We speculated that the effects of H19 in cardiomyocytes exposed to OGD/R may be mediated via miR-675 signaling. We transfected cardiomyocytes with si-H19, or with the combination of si-H19 and miR-675 mimic prior to OGD/R to investigate the effects of the H19/miR-675 axis on cell viability and apoptosis. Compared with transfection with si-H19 alone, the co-transfection of si-H19 and the miR-675 mimic significantly upregulated expression of miR-675 (Fig. 2A). As shown in Fig. 2B–D, OGD/R was found to be associated with reduced cell viability and elevated cell apoptosis. The transfection of si-H19 prior to OGD/R resulted in increased cell viability and decreased cell apoptosis, which was reversed by the co-transfection with si-H19 and miR-675 mimic, suggesting that H19 inhibition elevated cell viability and reduced cell apoptosis via inhibition of miR675 in cardiomyocytes exposed to OGD/R. Additionally, the expression of Caspase-3 and the Bax/Bcl-2 ratio increased markedly after OGD/R and decreased after transfection with si-H19. Compared with the si-H19 + OGD/R group, the expression of caspase-3 and Bax was upregulated, and the expression of Bcl-2 was downregulated in the si-H19 + miR-675 mimic + OGD/R group (Fig. 2E–H). Taken together, miR-675 could at least partially mediate the effects of H19 on cell viability and apoptosis in cardiomyocytes exposed to OGD/R.

3.3. The H19/miR-675 axis regulated inflammation and oxidative stress in cardiomyocytes exposed to OGD/R

The production of pro-inflammatory cytokines was measured by ELISA, as shown in Fig. 3A–C. IL-1β, TNF-a, and IL-6 significantly increased after exposure to OGD/R. Furthermore, si-H19 transfection reduced concentrations of these inflammatory cytokines, but the forced expression of miR-675 markedly increased them. Si-H19 transfection increased the production of anti-inflammatory cytokines IL-10 and TGF-β, which were decreased when miR-675 was overexpressed (Supplementary Fig. 2). Oxidative stress was assessed by detecting ROS and MDA levels and SOD activity. As shown in Fig. 3D–F, inhibition of H19 remarkably decreased OGD/R-induced increased ROS and MDA levels and elevated SOD activity. The attenuated oxidative stress caused by H19 inhibition was partly reversed by overexpression of miR-675. Furthermore, we measured the expression of proteins related to the inflammatory NF-κB signaling pathway and antioxidant Nrf2/HO-1 signaling pathway. The levels of p-IκB-α and p-p65 were upregulated and levels of Nrf2 and HO-1 were downregulated following the exposure to OGD/R. Inhibition of H19 was found to downregulate OGD/R-induced p-IκB-α and p-p65 levels and upregulate Nrf2 and HO-1 levels. The forced expression of miR-675 reversed these effects (Fig. 3G–I). Collectively, these data indicate that inhibition of H19/miR-675 could suppress OGD/R-induced inflammation and oxidative stress in cardiomyocytes, which may be closely associated with regulation of the NF-κB signaling pathway and Nrf2/HO-1 signaling pathway.

3.4. The H19/miR-675 axis negatively regulated PPARα

To investigate the mechanism underlying the effects of the H19/miR-675 axis, we used Miranda and TargetScan to predict the potential target genes of miR-675. We focused on PPARα, which belongs to

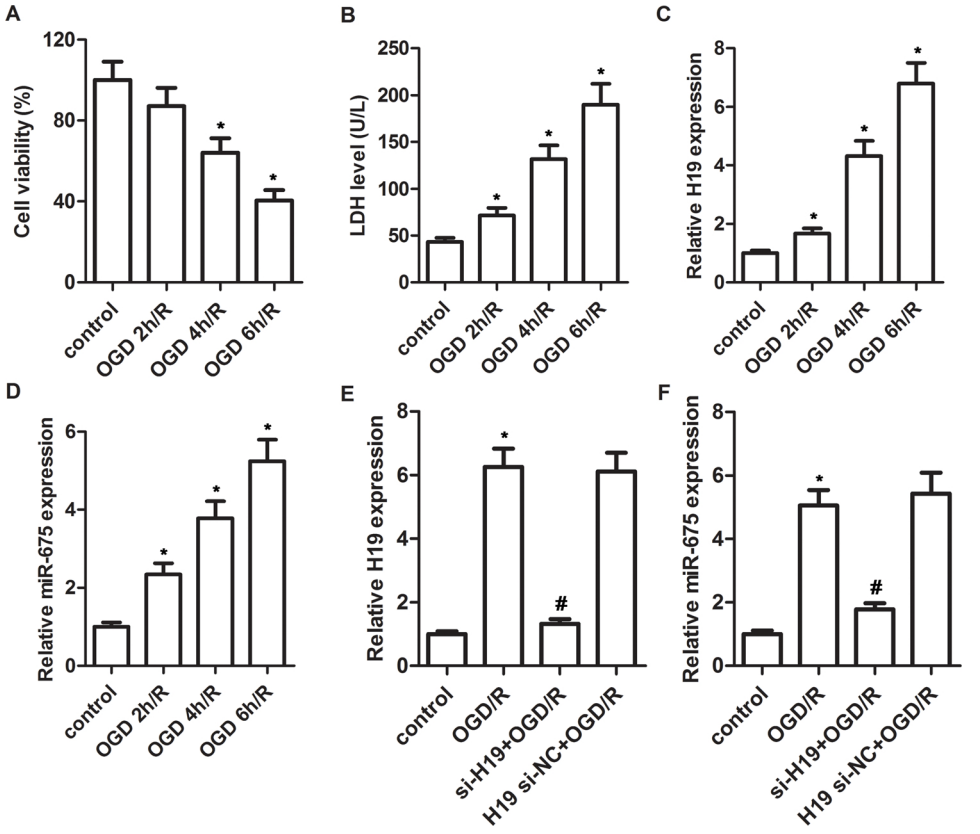

Fig. 1. Expression of H19 and miR-675 were upregulated in cardiomyocytes exposed to oxygen-glucose deprivation/reperfusion (OGD/R). Control represents the normal group; OGD 2 h/R, OGD 4 h/R, and OGD 6 h/R represent cardiomyocytes treated with 2 h, 4 h, and 6 h oxygen glucose deprivation, respectively, followed by 24 h reperfusion. (A) Cell viability was measured by CCK-8 assay. (B) LDH was measured using a LDH assay kit. (C) H19 was measured via qPCR and normalized to the expression of GAPDH. (D) MiR-675 was measured via qPCR and normalized to the expression of U6. Cardiomyocytes were then transfected with si-H19 or si-NC for 24 h prior to OGD 6 h/R. (E) H19 and (F) miR-675 were measured via qPCR. * $p < .05$ versus the control group, # $p < .05$ versus the OGD/R or H19 si-NC + OGD/R group.

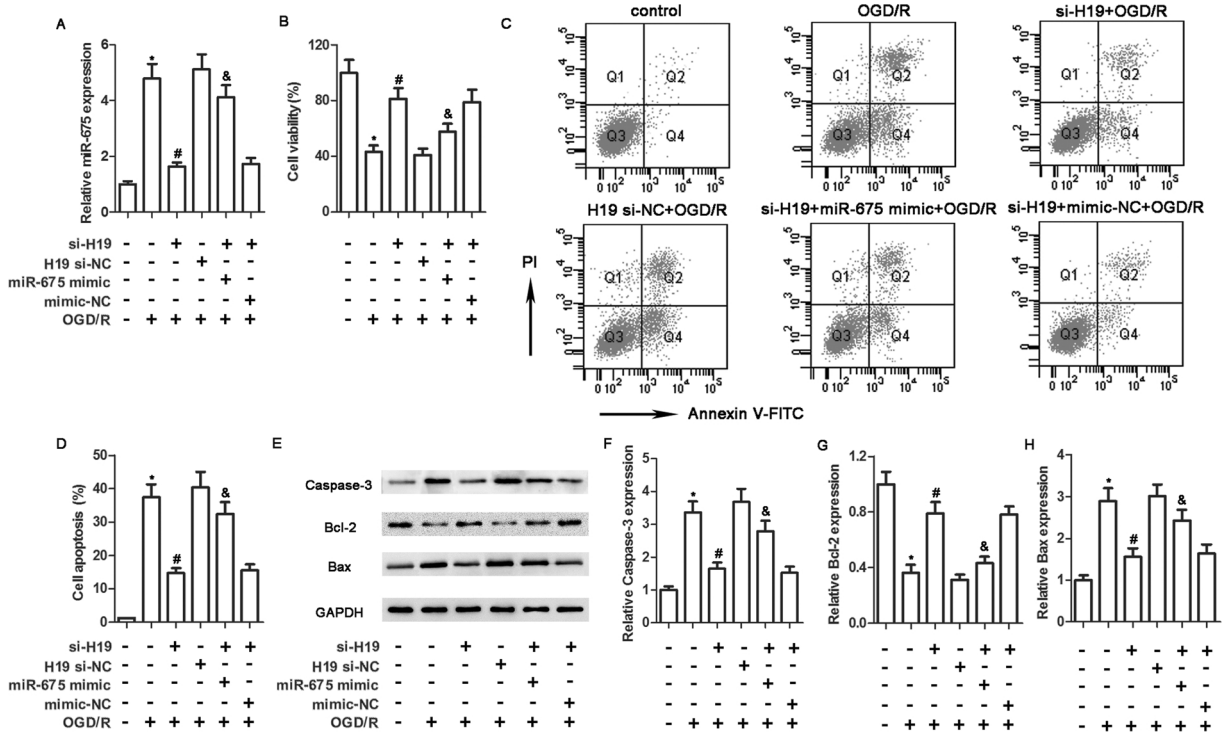

Fig. 2. Inhibition of H19 increased cell viability and reduced cell apoptosis in cardiomyocytes exposed to OGD/R via miR-675 inhibition. Cardiomyocytes were transfected with si-H19, si-NC, the combination of H19 and the miR-675 mimic, or the combination of H19 and the mimic-NC for 24 h prior to exposure to OGD 6 h/R. (A) MiR-675 was measured by qPCR. (B) Cell viability was measured by CCK-8 assay. Cell apoptosis was measured by (C) flow cytometry and is represented in a (D) histogram. (E) Expression of caspase-3, Bcl-2, and Bax was measured by western blot. The relative expression of (F) caspase-3, (G) Bcl-2, and (H) Bax is shown in a histogram. * $p < .05$ versus the control group, # $p < .05$ versus the OGD/R or H19 si-NC + OGD/R group, & $p < .05$ versus the si-H19 + OGD/R or si-H19 + mimic-NC + OGD/R group.

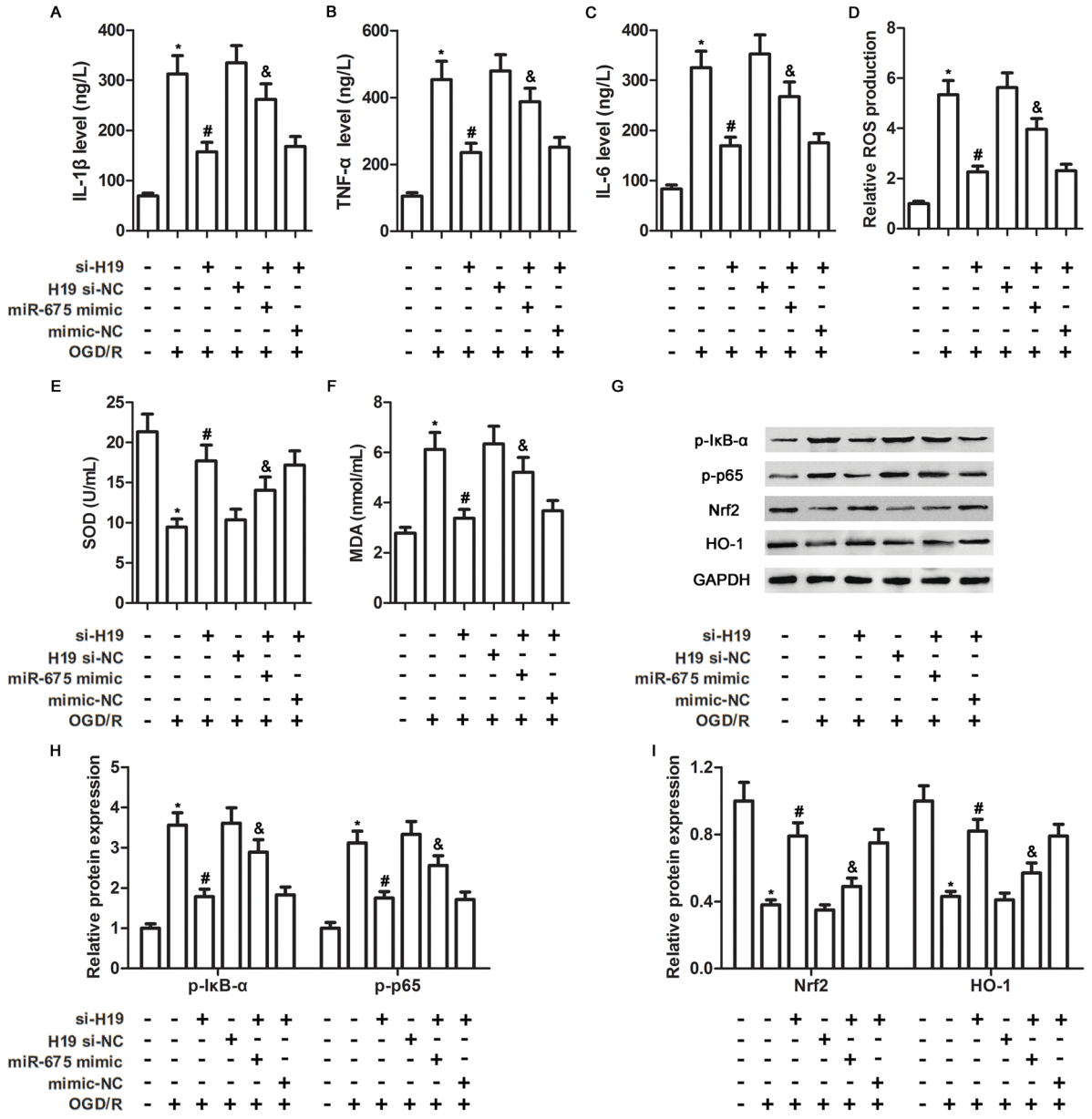

Fig. 3. Inhibition of H19 suppressed inflammation and oxidative stress in cardiomyocytes exposed to OGD/R via miR-675 inhibition. (A) IL-1β, (B) TNF-α, and (C) IL-6 in cell suspensions were detected by ELISA assay. (D) ROS production was measured by flow cytometry using DCHF-DA probes. Histograms indicate (E) SOD and (F) MDA levels. (G) The protein levels of p-IκB-α, p-p65, Nrf2, and HO-1 were measured by western blot. Histograms show the relative expression of (H) p-IκB-α and p-p65 and (I) Nrf2 and HO-1. * $p < .05$ versus the control group, # $p < .05$ versus the OGD/R or H19 si-NC + OGD/R group, & $p < .05$ versus the si-H19 + OGD/R or si-H19 + mimic-NC + OGD/R group.

ligand-activated transcription factors that reportedly play a crucial role in myocardial I/R injury (Ravingerová et al., 2009). Fig. 4A shows the predicted target sequences between miR-675 and PPARα. We cloned the 3′ UTR of PPARα mRNA (WT) or mutated 3′ UTR in the predicted miR-675 binding site (MUT) into luciferase reporter vectors and performed dual luciferase reporter assays. As shown in Fig. 4B, compared with the mimic-NC, the miR-675 mimic transfection decreased the activity of the firefly luciferase containing the 3′ UTR of PPARα by approximately 50%. However, miR-675 overexpression had no effect on the activity of firefly luciferase containing the mutant 3′ UTR of PPARα. The mRNA and protein expression of PPARα was downregulated in cardiomyocytes transfected with the miR-675 mimic, which was upregulated in cardiomyocytes transfected with the miR-675 inhibitor (Fig. 4C and D), indicating that miR-675 directly targeted the 3′ UTR of PPARα to suppress its expression. Moreover, the OGD/R treatment reduced the expression of PPARα, which was further decreased by miR-675 mimic transfection (Supplementary Fig. 3). We further found that inhibition of H19 significantly increased the OGD/R-mediated, reduced PPARα expression. MiR-675 overexpression partially reversed the effects of H19 inhibition, leading to the suppression of PPARα (Fig. 4E–G), suggesting that H19 negatively regulated PPARα via miR-675.

3.5. PPARα partly mediated the effects of the H19/miR-675 axis

We further investigated whether the effects of the H19/miR-675 axis in cardiomyocytes exposed to OGD/R were associated with the regulation of PPARα. The cardiomyocytes were transfected with miR-675 inhibitor, with the combination of miR-675 inhibitor and si-PPARα, or with the combination of si-H19 and si-PPARα. As shown in Fig. 5A, the co-transfection of si-PPARα significantly suppressed miR-675 inhibitor or si-H19 transfection-induced PPARα expression at the

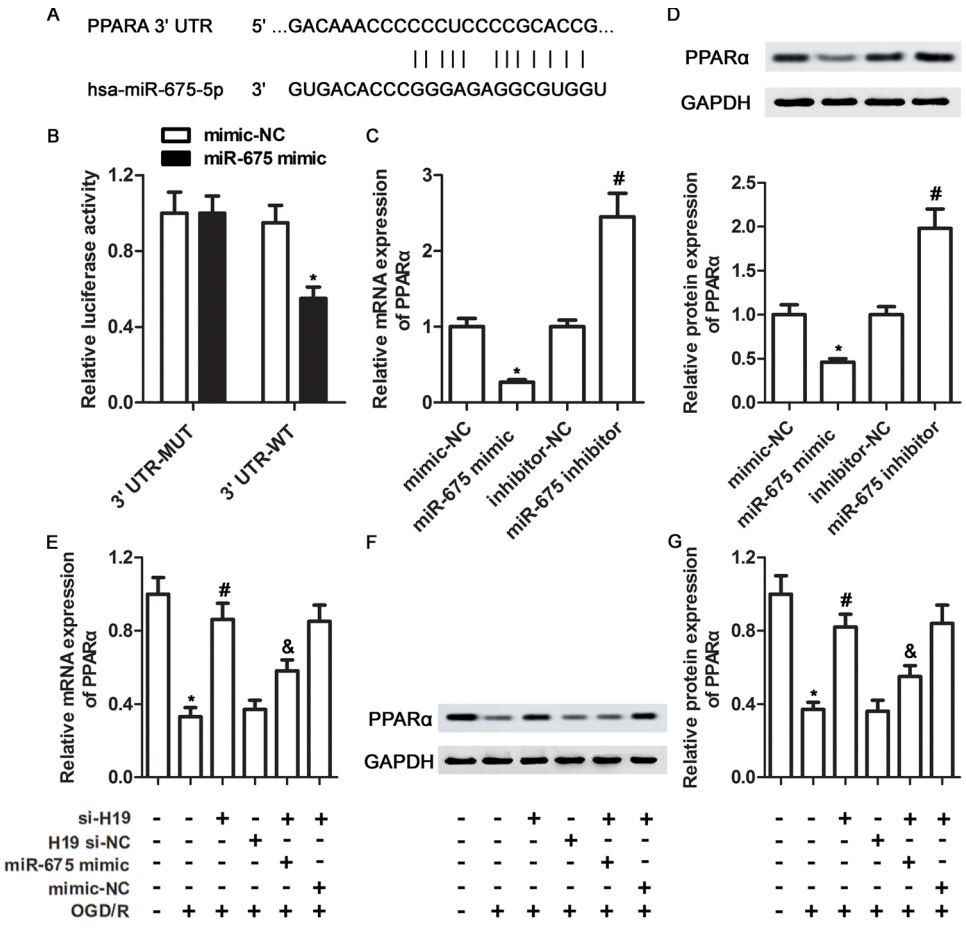

Fig. 4. The H19/miR-675 axis negatively regulated PPARα. (A) Predicted 3′ UTR sequence of PPARα in the miR-675 binding site. (B) The miR-675 mimic or mimic-NC were co-transfected into 293 T cells with the PPARα 3′ UTR (WT) or mutated PPARα 3′ UTR (MUT) reporter plasmids, along with a control Renilla luciferase pRL-TK vector. Luciferase activity was analyzed 48 h after transfection and normalized to Renilla luciferase activity. * $p <$ .05 versus the mimic-NC group. The (C) mRNA and (D) protein expression of PPARα in cardiomyocytes transfected with the miR-675 mimic or inhibitor was determined by qPCR and western blot, respectively. * $p <$ .05 versus the mimic-NC group, # $p <$ .05 versus the inhibitor-NC group. The (E) mRNA, and (F and G) protein expression of PPARα in cardiomyocytes transfected with si-H19 or the combination of H19 and miR-675 mimic was determined by qPCR and western blot, respectively. * $p <$ .05 versus the control group, # $p <$ .05 versus the OGD/R or H19 si-NC + OGD/R group, & $p <$ .05 versus the si-H19 + OGD/R or si-H19 + mimic-NC + OGD/R group.

mRNA levels. Furthermore, we again measured cell viability, cell apoptosis, inflammatory cytokine production, and oxidative stress and found that PPARα inhibition reversed the effects of miR-675 or H19 inhibition on those cell functions. Compared with the miR-675 inhibitor + OGD/R group or si-H19 + OGD/R group, in the miR-675 inhibitor + si-PPARα + OGD/R group and si-H19 + si-PPARα + OGD/R group, cell viability decreased; cell apoptosis increased; production of IL-1β, TNF-α, and IL-6 increased; ROS and MDA increased; and SOD activity was suppressed (Fig. 5B–I). These data indicate that PPARα may at least partially mediate the effects of the H19/miR-675 axis in cardiomyocytes exposed to OGD/R.

3.6. The H19/miR-675 axis regulated myocardial I/R injury in vivo

To verify the roles of the H19/miR-675/PPARα axis in vivo, we established a model of myocardial I/R using C57BL/6 mice. Mice were injected with adenoviruses harboring H19 siRNAs or H19 si-NC and then subjected to I/R. We found that H19 and miR-675 expression was upregulated, whereas PPARα expression was downregulated in the mice exposed to I/R (Fig. 6A–C). H19 knockdown resulted in downregulation of H19 and miR-675 but upregulation of PPARα, which was consistent with the in vitro data, indicating that the H19/miR-675/PPARα axis plays an important role in myocardial I/R injury. Furthermore, inhibition of H19 significantly reduced the I/R-induced infarct size (Fig. 6D), increased LVSP (Fig. 6E) and decreased LVEDP (Fig. 6F). These data indicate that H19 inhibition could markedly improve cardiac structure and function in myocardial I/R.

4. Discussion

Recently, increasing evidence has confirmed that the expression and function of H19 is closely associated with cancers, but its role in myocardial I/R injury has not been reported. In the present study, we established a cellular model of OGD/R and a mouse model of myocardial I/R to investigate the potential role of H19 in the pathogenesis of myocardial I/R. We found that H19 was upregulated in OGD/R-injured cardiomyocytes. Wang et al. have reported that H19 expression is upregulated in rats with cerebral I/R and in cells exposed to OGD/R. Inhibition of H19 protects cells against OGD/R-induced apoptosis, suggesting that H19 could be a new therapeutic target of ischemic stroke (Wang et al., 2017). In the present study, we found that H19 knockdown significantly protected cardiomyocytes from I/R injury, which was attributed to miR-675 generated from H19 RNA. Bioinformatic prediction and experimental analysis confirmed that miR-675 targeted PPARα. Our data thus provide a novel understanding of the role of the H19-miR-675–PPARα axis in myocardial I/R injury.

Apoptosis plays critical roles in the pathogenesis of myocardial I/R injury (Jr et al., 2004). During mitochondrial apoptosis, active cleaved caspase-3 increases, which contributes to the cleavage of cellular target proteins (Riedl and Shi, 2004). Bax and Bcl-2, two major Bcl-2 family members, are involved in the regulation of mitochondrial-mediated apoptosis (Youle and Strasser, 2008). Chen et al. have reported that overexpression of Bcl-2 attenuates apoptosis and protects against myocardial I/R injury in transgenic mice that carry a human Bcl-2 transgene (Chen et al., 2001). It also has been reported that inflammation and oxidative stress can mediate myocardial reperfusion injury (Yellon and Hausenloy, 2007). In the present study, we transfected cardiomyocytes with si-H19 or with the combination of si-H19 and miR-675 mimic prior to OGD/R to investigate the biological effects of the H19/miR-675 axis on cell apoptosis, inflammation, and oxidative stress. We found that knockdown of H19 decreased cell apoptosis; downregulated caspase-3 expression; upregulated the Bcl-2/Bax ratio;

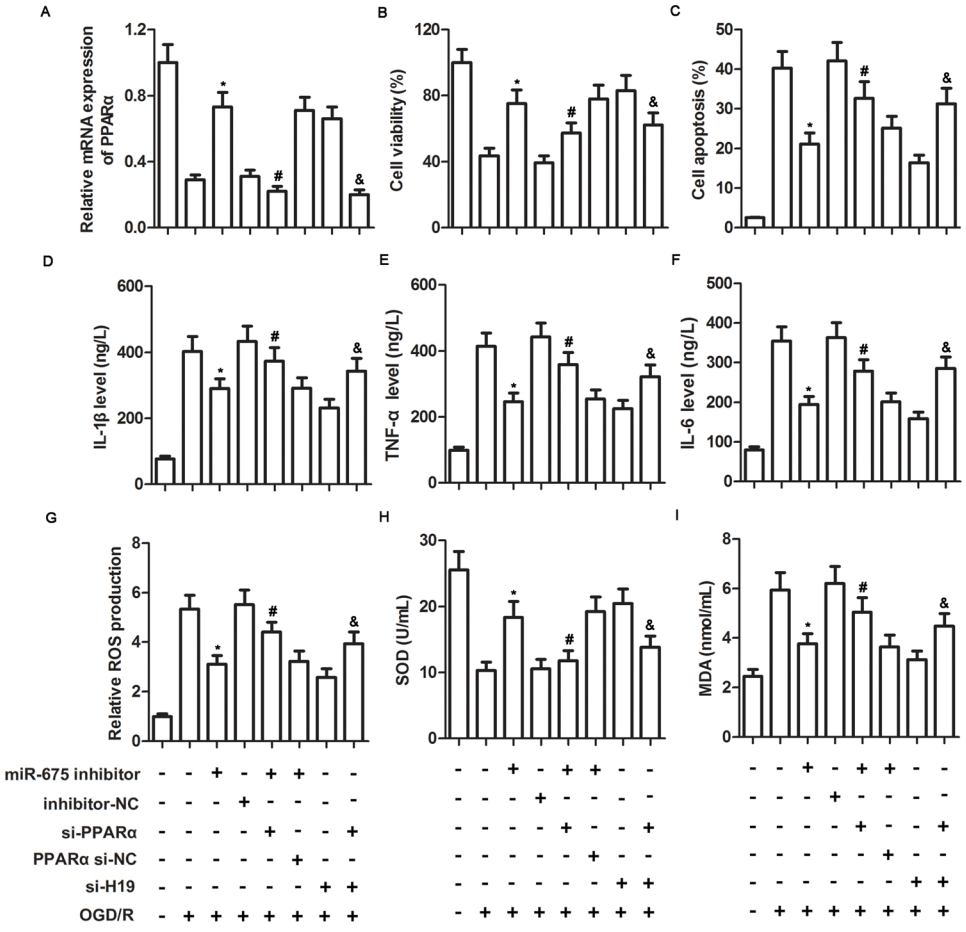

Fig. 5. PPARα partly mediated the effects of the H19/miR-675 axis. Cardiomyocytes were transfected with miR-675 inhibitor, with si-H19, with the combination of miR-675 inhibitor and si-PPARα, or with the combination of si-H19 and si-PPARα for 24 h prior to exposure to OGD 6 h/R. (A) The mRNA expression of PPARα was determined by qPCR. (B) Cell viability was measured by CCK-8 assay. (C) Cell apoptosis was measured by flow cytometry. (D) IL-1β, (E) TNF-α, and (F) IL-6 in cell suspensions were detected by ELISA assay. (G) ROS production was measured by flow cytometry using DCHF-DA probes. Histograms indicate levels of (H) SOD and (I) MDA. * $p < .05$ versus the OGD/R or inhibitor-NC + OGD/R group, # $p < .05$ versus the miR-675 inhibitor + OGD/R or miR-675 inhibitor + PPARα si-NC + OGD/R group, & $p < .05$ versus the si-H19 + OGD/R group.

reduced production of IL-1β, TNF-α, and IL-6; decreased ROS and MDA levels; elevated SOD activity; downregulated p-IκB-α and p-p65; and upregulated Nrf2 and HO-1. All of these effects could be reversed by the co-transfection with si-H19 and miR-675 mimic. These findings suggest that H19 knockdown protects cardiomyocytes against OGD/R injury, including apoptosis, inflammation, and oxidative stress, via miR-675 inhibition.

Moreover, it is well known that MDA is a marker of lipid peroxidation, which accumulation implies an iron-dependent form of regulated cell death-ferroptosis (Hong et al., 2017). The antioxidant

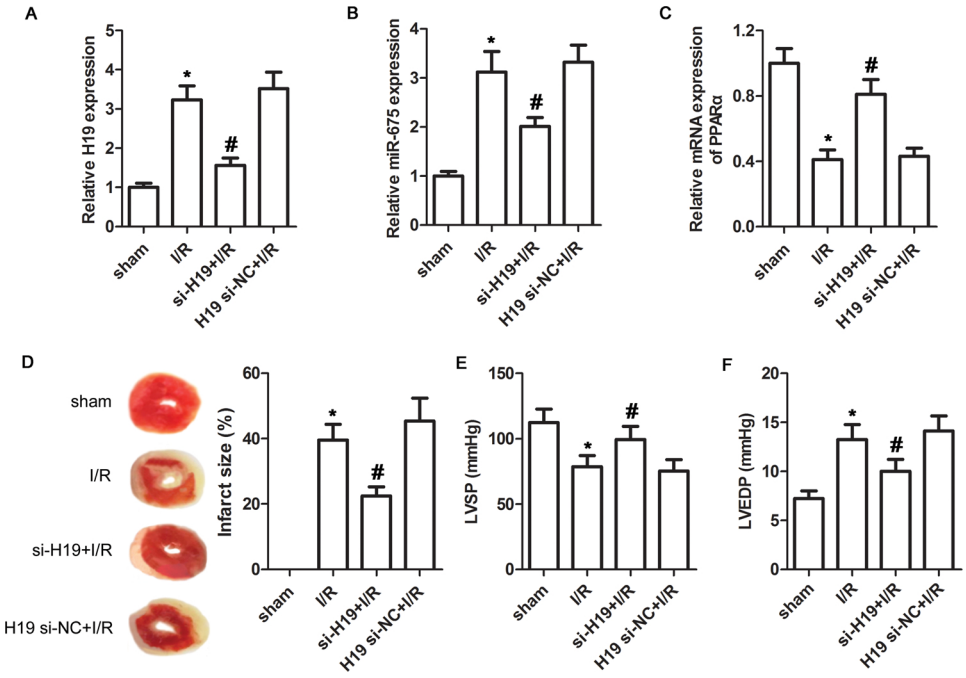

Fig. 6. The H19/miR-675 axis regulated myocardial I/R injury in vivo. C57BL/6 mice were injected with adenoviruses harboring H19 siRNAs or H19 si-NC, and then subjected to 45 min of ischemia and 1 week of reperfusion. Expression of (A) H19, (B) miR-675, and (C) PPARα was detected by qPCR, respectively. (D) The quantification of myocardial infarct volume by TTC staining. (E) Left ventricular systolic pressure (LVSP) and (H) left ventricular end-diastolic pressure (LVEDP). * $p < .05$ versus the sham group, # $p < .05$ versus the I/R or H19 si-NC + I/R group.

transcription factor Nrf2 regulates hundreds of genes, of which many are either directly or indirectly involved in modulating ferroptosis (Abdalkader et al., 2018). Among the genes, HO-1 is a major intracellular source of iron, and thus takes part in iron homeostasis and lipid peroxidation during ferroptosis (Adedoyin et al., 2017; Kwon et al., 2015). Therefore, the regulation of MDA, Nrf2 and HO-1 suggest that ferroptosis was involved in the actions of H19 in OGD/R injury. Inhibiting ferroptosis has been reported to represent a potential therapy for treating I/R-induced organ damage (Gao et al., 2015). Meanwhile, as a non-apoptotic form of cell death, ferroptosis was reported to be interrelated with apoptosis (Zheng et al., 2016). Recent studies reveal that ferroptosis-induced endoplasmic reticulum stress plays an important role in the crosstalk between ferroptosis and apoptosis (Hong et al., 2017; Lee et al., 2018). Thus, there must be a close link among oxidative stress, ferroptosis and apoptosis in the protection process of H19 knockdown against OGD/R injury, but the detailed molecular mechanisms still need more investigation.

H19 is a precursor of miR-675 that post-translationally modulates various target genes in different biological processes, such as cell proliferation, apoptosis, and differentiation (Dey et al., 2014; Gao et al., 2012; Li et al., 2016). We investigated the precise molecular mechanism of the H19-miR-675 axis in OGD/R injury. Using Miranda and TargetScan, we predicted the putative targets of miR-675, focusing on PPARα, which plays an important role in myocardial I/R injury (Johan et al., 2002; Yue et al., 2003). PPARα belongs to the nuclear receptor superfamily of ligand-activated transcription factors that regulate lipid and lipoprotein metabolism, glucose homeostasis, amino acid metabolism, inflammation, and cell differentiation (Desvergne and Wahli, 1999). PPARα has been implicated in potent anti-inflammatory activity through suppressing NF-κB signaling (Delerive et al., 2002, 2001; Smeets et al., 2007). NF-κB appears to play a causative role in inflammation, and it stimulates IL-6 expression in response to inflammatory signals. IL-6 may activate NF-κB, thereby completing a positive feedback loop, and it also affects other inflammatory cytokine production, such as IL-1β and TNF-α (Iliopoulos et al., 2009). PPARα has also been implicated in the expression or activation of anti-oxidant enzymes (Toyama et al., 2004). We confirmed by dual luciferase reporter assay that miR-675 directly targeted the 3′ UTR of PPARα to suppress its expression. Furthermore, we again measured cell viability, cell apoptosis, inflammatory cytokine production, and oxidative stress and found that PPARα inhibition reversed the effects of miR-675 and H19 inhibition on those cellular functions. These data indicate that PPARα may at least partially mediate the effects of the H19/miR-675 axis in cardiomyocytes exposed to OGD/R. Certainly, in an organism, or even a cell, the interactions between molecules are complex, either directly or indirectly. Other than miR-675, there should be other mechanisms for H19 to regulate PPARα expression. Meanwhile, H19 may play roles depending on other signaling, such as sponging let-7a/let-7b and miR-372/miR-373 (Wang et al., 2016). And H19/miR-675 axis may target a variety of gene mRNAs, such as VDAC1 (Li et al., 2016) and TGFBI (Zhu et al., 2015). Taken together, the detailed molecular mechanisms of H19 in OGD/R injury still need more investigation in the future.

To further verify the functional roles of the H19/miR-675/PPARα axis in vivo, we established a mouse model of myocardial I/R. Knockdown of H19 resulted in downregulation of H19 and miR-675 but upregulation of PPARα, which was consistent with the in vitro data. Moreover, knockdown of H19 in vivo significantly reduced I/R-induced infarction, increased LVSP, and decreased LVEDP. These data indicate that H19 inhibition could markedly improve cardiac structure and function in myocardial I/R. In summary, our study demonstrates that the H19/miR/675/PPARα axis played an important role in the pathogenesis of myocardial I/R injury, which provides new insights into understanding the molecular mechanisms of myocardial I/R. Targeting this axis could reveal a potential therapeutic strategy for I/R treatment.

Acknowledgement

This study was supported by Foundation of He' nan Educational Committee (15A320024).

Conflict of interest

The authors declare that they have no conflict of interest.

Appendix A. Supplementary data

Supplementary material related to this article can be found, in the online version, at doi:https://doi.org/10.1016/j.molimm.2018.11.011.

References

Abdalkader, M., Lampinen, R., Kanninen, K.M., Malm, T.M., Liddell, J.R., 2018. Targeting Nrf2 to suppress ferroptosis and mitochondrial dysfunction in neurodegeneration. Front. Neurosci. 12, 466.
Adedoyin, O., Boddu, R., Traylor, A.M., Lever, J.M., Bolisetty, S., George, J., Agarwal, A., 2017. Heme oxygenase-1 mitigates ferroptosis in renal proximal tubule cells. Am. J. Physiol. Renal Physiol. 314, F702–F714.
Cai, X., Cullen, B.R., 2007. The imprinted H19 noncoding RNA is a primary microRNA precursor. RNA 13, 313–316.
Chen, Z., Chua, C.C., Ho, Y.S., Hamdy, R.C., Chua, B.H., 2001. Overexpression of Bcl-2 attenuates apoptosis and protects against myocardial I/R injury in transgenic mice. Am. J. Physiol. Heart Circ. Physiol. 280, 2313–2320.
Delerive, P., De, B.K., Vanden, B.W., Fruchart, J.C., Haegeman, G., Staels, B., 2002. DNA binding-independent induction of IkappaBalpha gene transcription by PPARalpha. Mol. Endocrinol. 16, 1029–1039.
Delerive, P., Fruchart, J.C., Staels, B., 2001. Peroxisome proliferator-activated receptors in inflammation control. J. Endocrinol. 169, 453–459.
Desvergne, B., Wahli, W., 1999. Peroxisome proliferator-activated receptors: nuclear control of metabolism. Endocr. Rev. 20, 649–688.
Dey, B.K., Pfeifer, K., Dutta, A., 2014. The long noncoding RNA gives rise to microRNAs miR-675-3p and miR-675-5p to promote skeletal muscle differentiation and regeneration. Genes Dev. 28, 491–501.
Gabory, A., Jammes, H., Dandolo, L., 2010. The H19 locus: role of an imprinted noncoding RNA in growth and development. Bioessays News Rev. Mol. Cell. Dev. Biol. 32, 473.
Gao, Minghui, Monian, Prashant, Quadri, Nosirudeen, Ramasamy, Ravichandran, Jiang, Xuejun, 2015. Glutaminolysis and transferrin regulate ferroptosis. Mol. Cell 59, 298–308.
Gao, W.L., Liu, M., Yang, Y., Yang, H., Liao, Q., Bai, Y., Li, Y.X., Li, D., Peng, C., Wang, Y.L., 2012. The imprinted H19 gene regulates human placental trophoblast cell proliferation via encoding miR-675 that targets Nodal Modulator 1 (NOMO1). RNA Biol. 9, 1002.
Guan, G., Zhang, D., Wen, L., Xin, D., Liu, Y., Yu, D., Su, K., Zhu, L., Guo, Y., Wang, K., 2016. Overexpression of lncRNA H19/miR-675 promotes tumorigenesis in head and neck squamous cell carcinoma. Int. J. Med. Sci. 13, 914–922.
Hausenloy, D.J., Yellon, D.M., 2013. Myocardial ischemia-reperfusion injury: a neglected therapeutic target. J. Clin. Invest. 123, 92–100.
Hong, S.H., Lee, D.H., Lee, Y.S., Min, J.J., Jeong, Y.A., Kwon, W.T., Choudry, H.A., Bartlett, D.L., Yong, J.L., 2017. Molecular crosstalk between ferroptosis and apoptosis: emerging role of ER stress-induced p53-independent PUMA expression. Oncotarget 8, 115164–115178.
Iliopoulos, D., Hirsch, H.A., Struhl, K., 2009. An epigenetic switch involving NF-κB, Lin28, Let-7 MicroRNA, and IL6 links inflammation to cell transformation. Cell 139, 693–706.
Johan, A., Irina, C., Kristina, S., Laurence, J., Antonia, T., Ramaroson, A., 2002. Activation of the peroxisome proliferator-activated receptor α protects against myocardial ischaemic injury and improves endothelial vasodilatation. BMC Pharmacol. 2, 10.
Jr, H.J., Gilbert, T.B., Poston, R.S., Silldorff, E.P., 2004. Myocardial reperfusion injury: etiology, mechanisms, and therapies. J. Extra. Technol. 36, 391–411.
Kwon, M.Y., Park, E., Lee, S.J., Su, W.C., 2015. Heme oxygenase-1 accelerates erastin-induced ferroptotic cell death. Oncotarget 6, 24393–24403.
Lee, Y.S., Lee, D.H., Choudry, H.A., Bartlett, D.L., Lee, Y.J., 2018. Ferroptosis-induced endoplasmic reticulum stress: crosstalk between ferroptosis and apoptosis. Mol. Cancer Res molcanres.0055.2018.
Lewis, A., Lee, J.Y., Donaldson, A.V., Natanek, S.A., Vaidyanathan, S., Man, W.D., Hopkinson, N.S., Sayer, A.A., Patel, H.P., Cooper, C., et al., 2016. Increased expression of H19/miR-675 is associated with a low fat-free mass index in patients with COPD. J. Cachexia Sarcopenia Muscle 7, 330–344.
Li, X., Wang, H., Yao, B., Xu, W., Chen, J., Zhou, X., 2016. lncRNA H19/miR-675 axis regulates cardiomyocyte apoptosis by targeting VDAC1 in diabetic cardiomyopathy. Sci. Rep. 6, 36340.
Liao, Y.H., Xia, Ni, Zhou, Su-Feng, Tang, Ting-Ting, Yan, Xin-Xin, Lv, Bing-Jie, Nie, Shao-Fang, Wang, Jing, Yoichiro, Iwakura D., Xiao, Hong, et al., 2016. Interleukin-17A contributes to myocardial ischemia/reperfusion injury by regulating cardiomyocyte apoptosis and neutrophil infiltration. J. Am. Coll. Cardiol. 149, 10–17.

Ong, S.B., Katwadi, K., Kwek, X.Y., Ismail, N.I., Ong, S.G., Chinda, K., Hausenloy, D.J., 2018. Non-coding RNAs as therapeutic targets for preventing myocardial ischemia-reperfusion injury. Expert Opin. Ther. Targets 22, 247–261.
Ravingerová, T., Adameová, A., Kelly, T., Antonopoulou, E., Pancza, D., Ondrejcáková, M., Khandelwal, V.K., Carnická, S., Lazou, A., 2009. Changes in PPAR gene expression and myocardial tolerance to ischaemia: relevance to pleiotropic effects of statins. Can. J. Physiol. Pharmacol. 87, 1028–1036.
Riedl, S.J., Shi, Y., 2004. Molecular mechanisms of caspase regulation during apoptosis. Nat. Rev. Mol. Cell Biol. 5, 897–907.
Smeets, P.J., Planavila, A., Gj, V.D.V., Van, B.M., 2007. Peroxisome proliferator-activated receptors and inflammation: take it to heart. Acta Physiol. 191, 171–188.
Toyama, T., Nakamura, H., Harano, Y., Yamauchi, N., Morita, A., Kirishima, T., Minami, M., Itoh, Y., Okanoue, T., 2004. PPARalpha ligands activate antioxidant enzymes and suppress hepatic fibrosis in rats. Biochem. Biophys. Res. Commun. 324, 697–704.
Tsang, W.P., Ng, E.K.O., Ng, S.S.M., Jin, H., Yu, J., Sung, J.J.Y., Kwok, T.T., 2010. Oncofetal H19-derived miR-675 regulates tumor suppressor RB in human colorectal cancer. Carcinogenesis 31, 350.
Vennin, C., Spruyt, N., Dahmani, F., Julien, S., Bertucci, F., Finetti, P., Chassat, T., Bourette, R.P., Le Bourhis, X., Adriaenssens, E., 2015. H19 non coding RNA-derived miR-675 enhances tumorigenesis and metastasis of breast cancer cells by down-regulating c-Cbl and Cbl-b. Oncotarget 6, 29209–29223.
Wang, J., Cao, B., Han, D., Sun, M., Feng, J., 2017. Long non-coding RNA H19 induces cerebral ischemia reperfusion injury via activation of autophagy. Aging Dis. 8, 71.
Wang, J.X., Zhang, X.J., Li, Q., Wang, K., Wang, Y., Jiao, J.Q., Feng, C., Teng, S., Zhou, L.Y., Gong, Y., 2015a. MicroRNA-103/107 regulate programmed necrosis and myocardial ischemia/reperfusion injury through targeting FADD. Circ. Res. 117, 352.
Wang, K., Liu, C.Y., Zhou, L.Y., Wang, J.X., Man, W., Bing, Z., Zhao, W.K., Xu, S.J., Fan, L.H., Zhang, X.J., 2015b. APF lncRNA regulates autophagy and myocardial infarction by targeting miR-188-3p. Nat. Commun. 6, 6779.
Wang, W.T., Ye, H., Wei, P.P., Han, B.W., He, B., Chen, Z.H., Chen, Y.Q., 2016. LncRNAs H19 and HULC, activated by oxidative stress, promote cell migration and invasion in cholangiocarcinoma through a ceRNA manner. J. Hematol. Oncol. 9, 117.
Yellon, D.M., Hausenloy, D.J., 2007. Myocardial reperfusion injury. N. Engl. J. Med. 357, 1121–1135.
Youle, R.J., Strasser, A., 2008. The BCL-2 protein family: opposing activities that mediate cell death. Nat. Rev. Mol. Cell Biol. 9, 47–59.
Yue, T., Bao, W., Beat, M., Gu, J., Romanic, A., Brown, P., Cui, J., Thudium, D., Boyce, R., Burns-Kurtis, C., Mirabile, R., 2003. Activation of peroxisome proliferator-activated receptor-alpha protects the heart from ischemia/reperfusion injury. Circulation 108, 2393–2399.
Zhao, Z.H., Hao, W., Meng, Q.T., Du, X.B., Lei, S.Q., Xia, Z.Y., 2017. Long non-coding RNA MALAT1 functions as a mediator in cardioprotective effects of fentanyl in myocardial ischemia-reperfusion injury. Cell Biol. Int. 41, 62–70.
Zheng, D.W., Lei, Q., Zhu, J.Y., Fan, J.X., Li, C.X., Li, C., Xu, Z., Cheng, S.X., Zhang, X.Z., 2016. Switching apoptosis to ferroptosis: metal–organic network for high-efficiency anticancer therapy. Nano Lett. 17, 284–291.
Zhu, M., Chen, Q., Liu, X., Sun, Q., Zhao, X., Deng, R., Wang, Y., Huang, J., Xu, M., Yan, J., 2014. lncRNA H19/miR-675 axis represses prostate cancer metastasis by targeting TGFBI. FEBS J. 281, 3766–3775.
Zhu, M., Chen, Q., Liu, X., Sun, Q., Zhao, X., Deng, R., Wang, Y., Huang, J., Xu, M., Yan, J., 2015. lncRNA H19/miR-675 axis represses prostate cancer metastasis by targeting TGFBI. FEBS J. 281, 3766–3775.